

INVESTIGATIONS OF DEFECT CENTRES IN ALKALI HALIDES DOPED WITH TRIVALENT CATIONS. PART 1: BISMUTH IN NaCl, KCl AND RbCl CRYSTALS

M. SUSZYŃSKA

W. Trzebiatowski Institute of Low Temperature and Structure Research
Polish Academy of Sciences
Pl. Katedralny 1, 50-950 Wrocław, Poland

AND R. CAPELLETTI

Physics Department, Parma University, 43100 Parma, Italy

Dedicated to Professor Dr. Julian Auleytner
on the occasion of his 70th birthday

(Received July 9, 1992)

A correlated set of experiments was performed with a view to study the effect of trivalent bismuth upon some properties of NaCl, KCl and RbCl crystals. For NaCl the effect of BiO^+ ions was also investigated. It was stated that: 1. The hydrolytic properties of bismuth are responsible for the formation of BiO^+ centres also in crystals doped with Bi^{3+} ions. 2. During all experiments performed, the dopant remains in the form of trivalent cations. 3. Optical absorption spectra of bismuth are similar to those characteristic of other heavy metal ions with the s^2 electronic configuration. 4. The charge excess of Bi^{3+} ions is compensated by cation vacancies whereas for BiO^+ ions the preferential bonding between Bi^{3+} and O^{2-} serves for the charge compensation.

PACS numbers: 77.40.+i

1. Introduction

Many papers have reported the effect of impurities upon different physical properties of alkali halide (AH) crystals. Most of these works dealt with divalent cations (Me^{2+}) present in sodium and potassium chlorides. Only few experiments

have been performed on crystals doped with trivalent impurities (Me^{3+}). The significance of these works relates, among others, with a renewed interest in spectroscopic properties of simple salts doped with elements with the *d*- and *f*-electrons.

Dielectric properties of trivalent cations in monovalent ionic crystals, like alkali- and silver halides, were up to now studied by various authors [1–5]. According to Kunze et al. [5] such ions as Ti^{3+} , Cr^{3+} and V^{3+} enter substitutionally the monovalent lattice of AgCl and at sufficiently low temperature are completely associated with two cation vacancies. These complexes are able to reorient by a thermally activated jump of one of the species involved. Like the impurity–vacancy (I.V.) dipoles in $\text{AH}:\text{Me}^{2+}$ systems, the pertinent defects in the Me^{3+} doped crystals have been assigned *impurity–vacancy–vacancy* (I.V.V.) *dipoles*.

To obtain further information about the composed character of the mentioned defects and their configuration within the matrix, about the number and distribution of the excess charge compensating cation vacancies etc., bismuth doped NaCl, KCl and RbCl crystals (Part 1) and chromium doped NaCl crystals (Part 2) were studied by means of ionic thermocurrent (ITC) technique. These measurements were complemented by investigations of some spectroscopical, electric and mechanical characteristics. It should be noted that the ionic radius of these trivalent cations is smaller than that of the host cations and the geometrical situation in the $\text{AH}:\text{Me}^{3+}$ systems studied resembles that of silver halides doped with trivalent impurities [5].

2. Experimental details

2.1. Origin of crystals and the dispersion state of the dopant

The crystals were grown by Dr M. Lebl from Scientific Service in Prague (Czecho-Slovakia) according to a modified Bridgman method [6]; for basic characteristics of the samples see Table I. As received (AR) crystals were used mainly. To modify the state of aggregation of the dopant, AR samples were annealed at 873 K for various times; the multiply of 30 minutes was employed. After each period of annealing, the hot sample was dropped onto a copper plate at room temperature (RT). This procedure defines the solution treated (ST) state of impurities. In some instances the effect of uniaxial compression (along a $\langle 100 \rangle$ direction) was investigated. The deformation was realized in a self-made device with load calibrated against the 1112 INSTRON machine working at a strain rate equal to $3 \times 10^{-4} \text{ s}^{-1}$.

2.2. Valency of bismuth

When bismuth enters the crystal lattice in a trivalent state, no paramagnetism is expected as the outer electronic configuration is $6s^2$, whereas if it is in the divalent state, associated paramagnetic behaviour occurs. EPR spectroscopy was used to characterize and to verify the valency of the dopant in both as received as well as thermally and mechanically pretreated samples. The spectra were taken at RT and liquid nitrogen temperature (LNT) with the VARIAN-V-4502 spectrometer. Independently of the crystal matrix, type and concentration of the dopant

TABLE I
Basic characteristics of the crystals.

System	Mark	c [mppm]*	α [cm ⁻¹]**	
NaCl:Bi(3+)	D.1	50	0.38	
	2	100	1.52	
	3	1000	0.81	
	4	1000	5.01	
	6	5000	2.97	
	NaCl:BiO(+)	E.2	50	1.12
4		100	0.52	
5		1000	8.01	
6		2000	14.82	
7		5000	1.62	
8		10000	17.62	
9		1000	2.16	
10		800	4.61	
KCl:Bi(3+)		M.1	1000	3.90
		2	1000	20.71
RbCl:Bi(3+)	R.1	1000	—	

*Dopant concentration in the melt.

**Absorption coefficient of the high-energy band $\alpha^C/\alpha^A \cong 4.5, 4.3$ and 7 for E, D and M crystals respectively.

and the pretreatment of samples, no EPR signal related with divalent bismuth was registered.

Preliminary studies of the mechanical characteristics permitted also to exclude the presence of monovalent bismuth ions, in the NaCl crystals at least. Figure 1 shows the concentration dependence of Vickers microhardness taken at 0.1 N for Bi³⁺- (curve *a*) and BiO⁺- (curve *b*) doped AR samples. The impurity induced strengthening of slightly doped crystals is followed by a relative softening of samples with the largest amount of the dopant. Both phenomena are explainable in the frame of elastic interactions between moving dislocations and tetragonal strain fields related with the impurity obstacles [7, 8]. For monovalent impurities, located substitutionally in the NaCl matrix, the local symmetry of the induced strain fields should remain cubic, presenting much less effective obstacles for the moving dislocations.

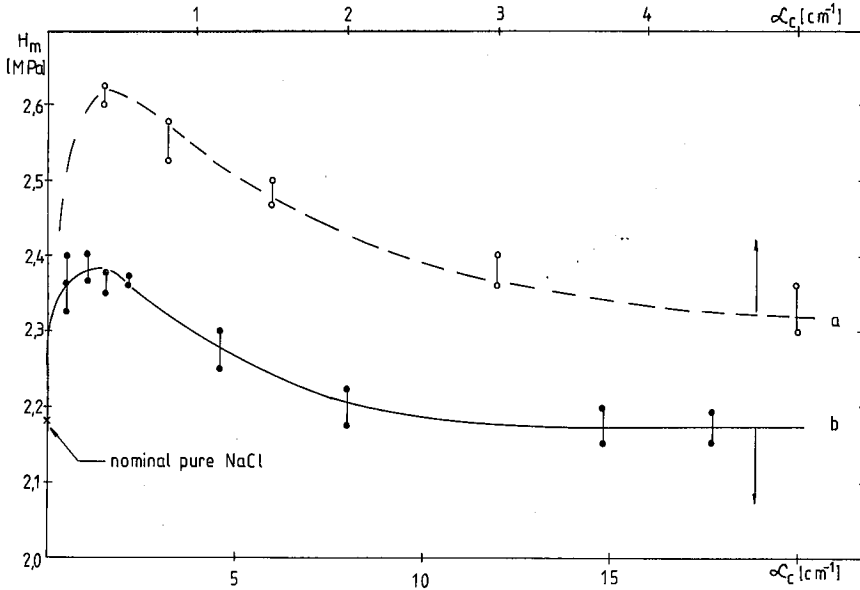


Fig. 1. Concentration dependences of the Vickers microhardness for bismuth doped NaCl crystals; curves *a* and *b* concern Bi(3+) and BiO(+) doped crystals, respectively; the concentration is represented by the absorption coefficient value of the *C* band.

2.3. Other measurements performed

Optical absorption spectra were measured between 195 and 800 nm by means of a SPECORD (Zeiss) spectrophotometer. Conductivity data were obtained by taking the resistance of samples subjected to 100 V of dc; a GENERAL RADIO 1621 bridge was used for these measurements. To avoid polarization effects the dc voltage was applied for a short time to crystal faces coated with colloidal graphite. Dielectric relaxation phenomena were studied by measuring thermally stimulated depolarization currents (ITC) according to the procedure developed by Bucci et al. [9]. The measurements were usually performed in an extended range of testing temperature (LNT–373 K). For plastically deformed samples the measurement arrangement has been described elsewhere [10].

3. Results and discussion

3.1. Analysis of the absorption data

3.1.1. Absorption spectra

Figures 2 and 3 show some examples of the optical absorption spectra of bismuth doped crystals, and Table II lists the positions of bands detected at RT and LNT. Three bands (*A*, *B*, *C*) were usually observed, from which the *C* band exhibits a more or less distinct structure when measured at LNT; these findings are

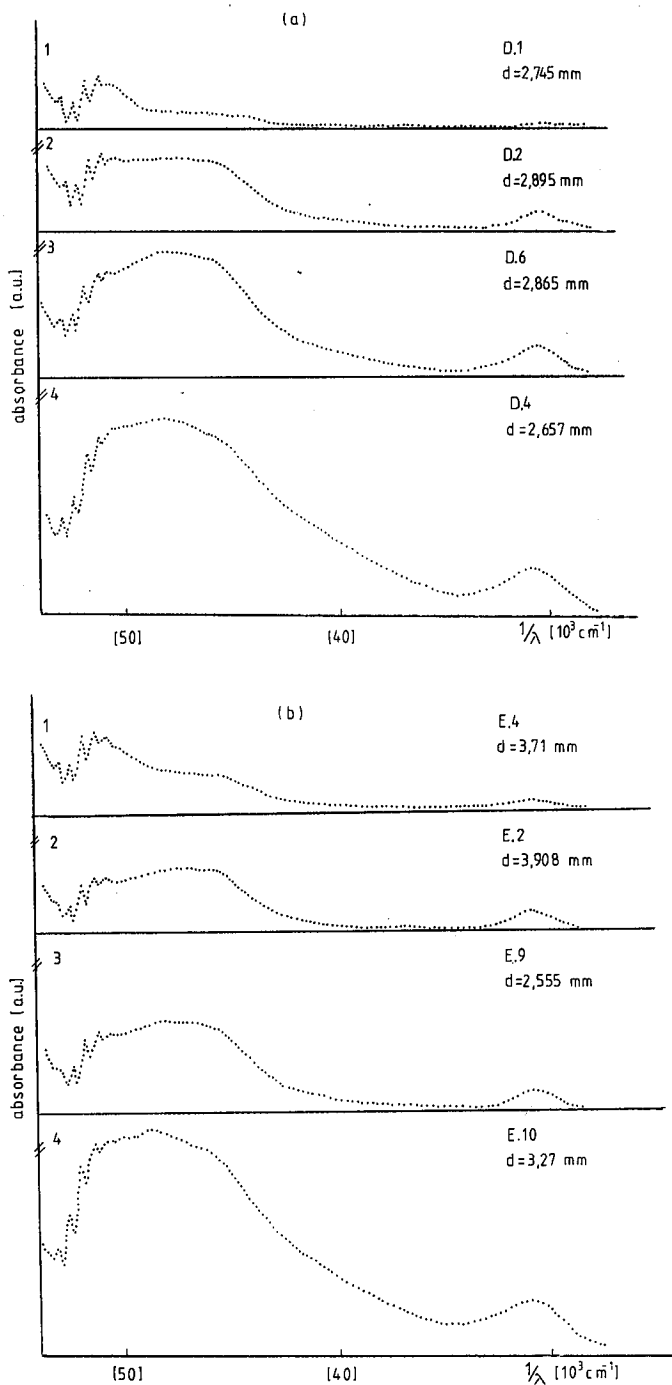


Fig. 2. Optical absorption spectra of NaCl crystals doped with various amounts of Bi^{3+} (a) and BiO^+ (b) ions.

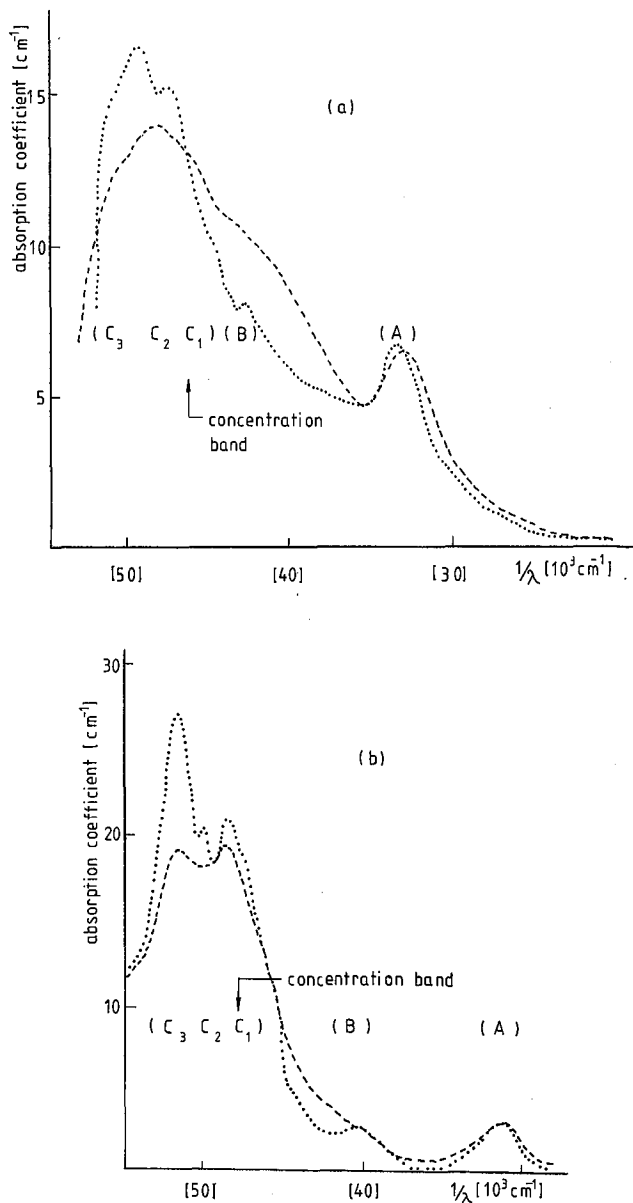


Fig. 3. Optical absorption of E.6 (a) and M.2 (b) crystals measured at RT (—) and LNT (•); for the first spectrum the α^C/α^A ratio is equal only to 2.18.

essentially consistent with the literature data. Some peculiarities registered were as follows.

For both types of the dopant in NaCl crystals the spectra exhibit some dif-

TABLE II
Positions of the absorption bands induced by bismuth in the alkali halide crystals.

System	A-band		B-band	$C_1 \div C_2$
	RT	LNT	LNT	LNT
D	328	325	240	195÷212
E	320	320	—	195÷213
M	330	325	244	201÷212

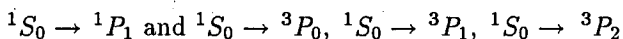
ferences with respect to the testing temperature. At LNT, for instance, a shift of the position of the lowest-energy band (*A*) towards shorter wavelengths and the absence of the next band (*B*) were detected for crystals nominally doped with Bi^{3+} and BiO^+ ions, respectively. For both dopants the bands observed at 195 nm are probably related with the presence of some oxygen-containing centres. The preferential bonding between Bi^{3+} and O^{2-} assures the excess charge compensation in BiO^+ centres. Annealing of solution treated samples at temperatures up to about 573 K yields a decrease in the intensity of the *A* and *C* bands. The ratio of the absorption coefficients α^A/α^C is only slightly larger for the BiO^+ doped samples. Similar behaviour of both bands speaks in favour of the fact that they are related with the same type of optically active centres.

For $\text{KCl}:\text{Bi}^{3+}$ crystals the *B* band as well as the structure of the *C* band disappear when the testing temperature increases above 80 K. Moreover, the solution treatment induces a shift of the *A* band towards longer wavelengths.

For $\text{RbCl}:\text{Bi}^{3+}$ crystals no optical absorption was detected all over the UV spectral range for samples as thick as about 2.5 mm; for thicker samples an absorption trace was registered between 280 and 330 nm. These facts are probably consequences of an extremely low solubility limit of trivalent bismuth in the rubidium salts.

3.1.2. Determination of dopant concentration

General features of the absorption spectra obtained are similar to those characteristic of other alkali halides containing small amount of heavy metal ions with the mercury-like s^2 configuration, see for instance the work by Fukuda [11]. Thus, the pertinent absorption bands should correspond to the following transitions:



in the impurity cations, whose levels are perturbed by the crystal field. Exploiting this similarity, bismuth concentration was calculated from the Smakula equation describing the relationship between the number N of optically active centres per cm^3 and the absorption coefficient a^C of the *C* band. Taking for the parameters in this equation: 0.5 for the oscillator strength f^C [11], 1.8 for refractive index $n(\text{RT})$ at 200 nm, 0.74 eV for the band half-width $W_{1/2}^C$, the values of N (in mole ppm)

ranged between 0.14 and 1.91 for Bi^{3+} - and between 0.19 and 6.74 for BiO^+ doped NaCl. Similar calculations, performed for KCl ($n \cong 1.719$ and $W_{1/2}^C \cong 0.87$), yield N equal to 2.56 and 13.63 mppm for the samples studied.

3.2. Ionic conductivity

3.2.1. $\sigma(T)$ plot

Figure 4 shows the temperature dependence of conductivity σ of NaCl and KCl crystals doped with BiO^+ and Bi^{3+} , respectively. For the sake of comparison the σT vs. $(1/T)$ plots for nominally pure (with few ppm of divalent impurities) NaCl and KCl as well as for KCl:Pb^{2+} crystals are also presented. These dependencies display two weakly expressed regions, the extrinsic and the association one. Similar to Me^{2+} ions, the larger the dopant concentration, the higher the temperature at which association with vacancies occurs. Estimated values of the association energy are nearly equal to 0.68 eV, which differs considerably from the value characteristic of divalent impurities, cp. [12, 13].

3.2.2. Solubility of bismuth and the excess charge compensation

According to Stoicescu et al. [14] it is not easy to obtain the alkali halide crystals with a large amount of trivalent cations. This fact is in contrast to the situation in AH:Me^{2+} crystals for which the dopant solubility increases with decreasing ionic radius of the impurity. It seems reasonable to suppose that for the trivalent cations the increasing difference in valency between the substituted and the substituting cations yields a decrease in both the solubility limit of the dopant and the stability of the solid solution formed. Although the co-presence of some aliovalent anions should affect both mentioned quantities, the effect of O^{2-} inferred from the absorption data, for instance, is not clear from the plots of electrical conductivity. It can be seen, for instance, that for the BiO^+ doped NaCl crystals the conductivity is practically independent of the presence of the dopant. When — similar to silver halides [5] — bismuth ions enter the lattice of alkali halides substitutionally, each impurity ion should be accompanied by two cation vacancies. Then, neglecting the number of intrinsic defects, the conductivity characteristic of the association region should be for trivalent cations twice as large as for the divalent ones. Moreover, the association with cation vacancies should start at higher temperatures and the electrostatic interactions should be stronger in the case of Me^{3+} doped alkali halides than for the Me^{2+} doped crystals for which only one cation vacancy is involved. Although some of these phenomena were detected experimentally, see Fig. 3, low solubility of bismuth makes the quantitative analysis of the obtained results difficult. Among others, the problem related with the number of excess charge compensating vacancies remains open. The difference in the association energy values, related to di- and trivalent cations, could be understood if one assumes that only one cation vacancy is tightly bounded with the trivalent cation. The second vacancy should be located at a position further than the next nearest neighbour one and bound with much less energy. For this and other reasons, it seems necessary to compare data obtained for di- and trivalent cations of chemically the same element.

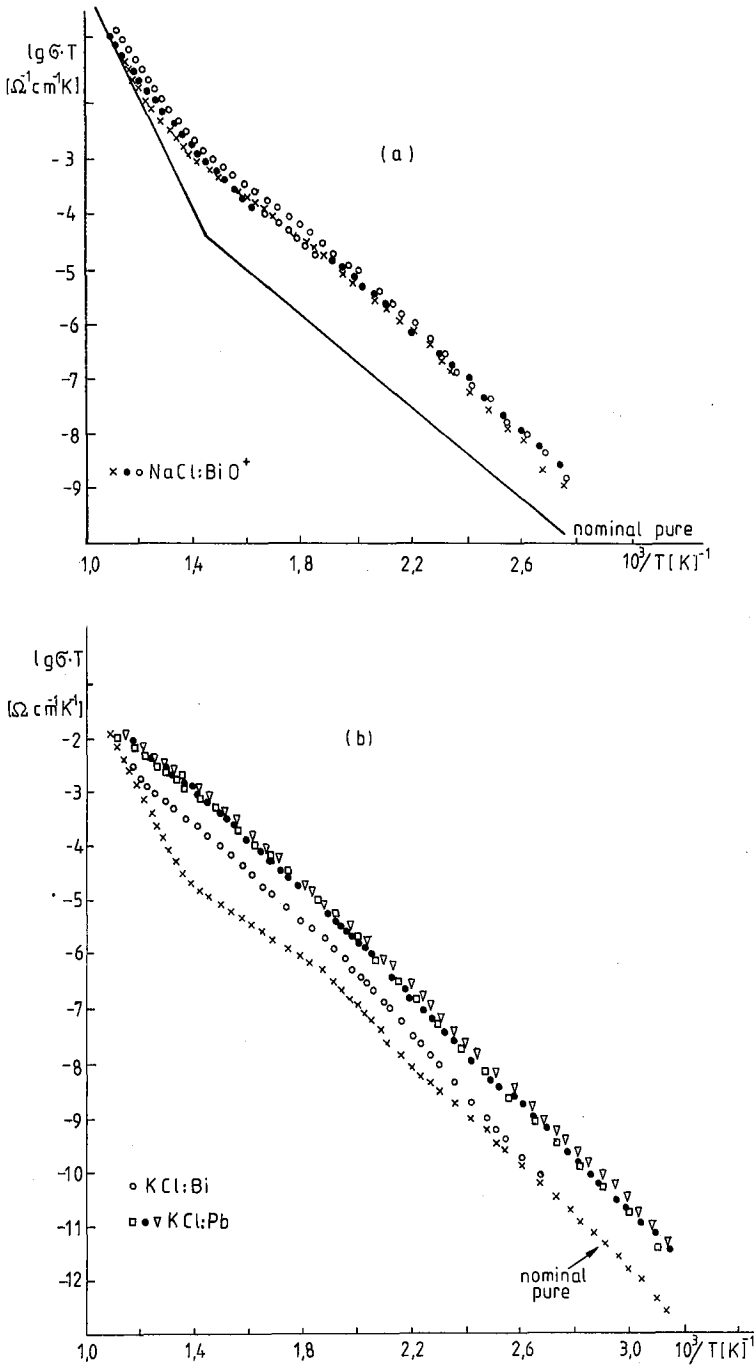


Fig. 4. Temperature dependence of electric conductivity of E (a) and M (b) crystals; in (b) the data characteristic of $\text{KCl}:\text{Pb}(2+)$, according to [12], are also presented.

3.3. ITC data

3.3.1. AR state

For plate-shaped AR samples at least one low- (*A*) and one high-temperature (*C*) ITC band were observed; Figs. 5–8 show some examples of the data obtained. The low-temperature band is already present in AR samples, and its amplitude H^A reacts to the polarizing field E_p in a way similar to the dipole band in AH:Me²⁺ systems, e.g. [10]. For KCl:Bi³⁺ crystals the band also reacts to the polarizing temperature T_p resembling the behaviour of the low-temperature band in the LiF:Ti³⁺ system [1]. Moreover, in all cases the *A* band is positioned below the dipole band characteristic of divalent impurities in alkali halides. The linearity of the $H^A(E_p)$ dependence and relatively weak polarizations related with this band are consistent with the main features of dielectric relaxations induced by low concentrations of non-interacting dipolar defects. Although the geometrical model of such defects is not univocally known for trivalent cations, the concept of I.V.V.

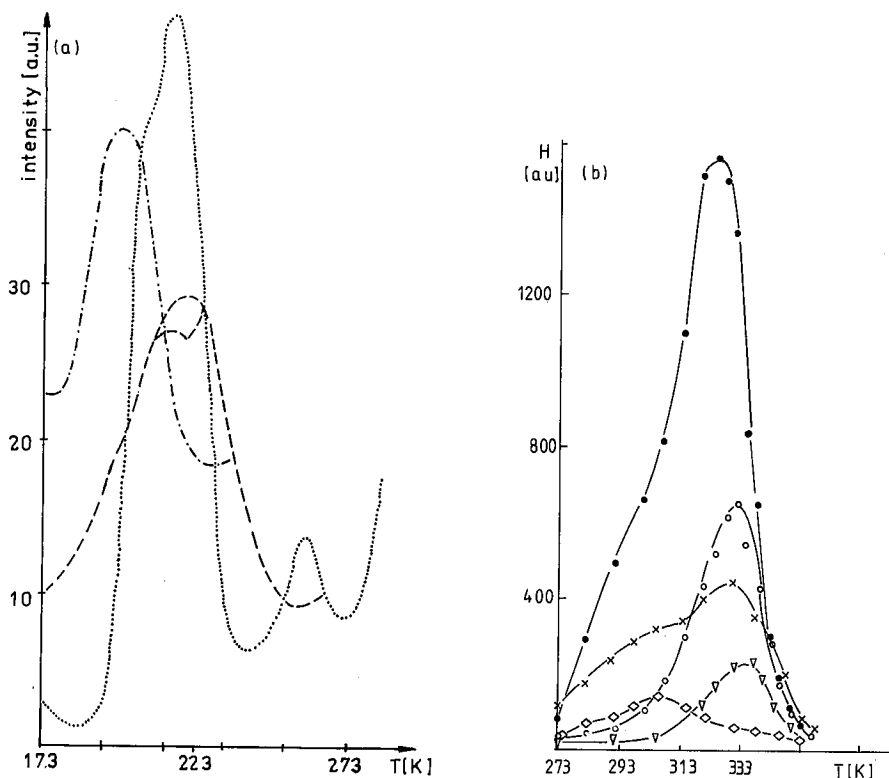


Fig. 5. ITC of crystals in the (a) low- and (b) high-temperature range; polarization conditions for all samples: $T_p \cong RT$, $T_l = 178$ K, $V_p = 10^3$ V. Spectra of the following crystals are shown: for (a) E.11 (\bullet), M.1 (---) and R.1 (—), for (b) E.11 (o), E.8 (\bullet), M.1 (\square), R.1 (∇) and D.2 (\times).

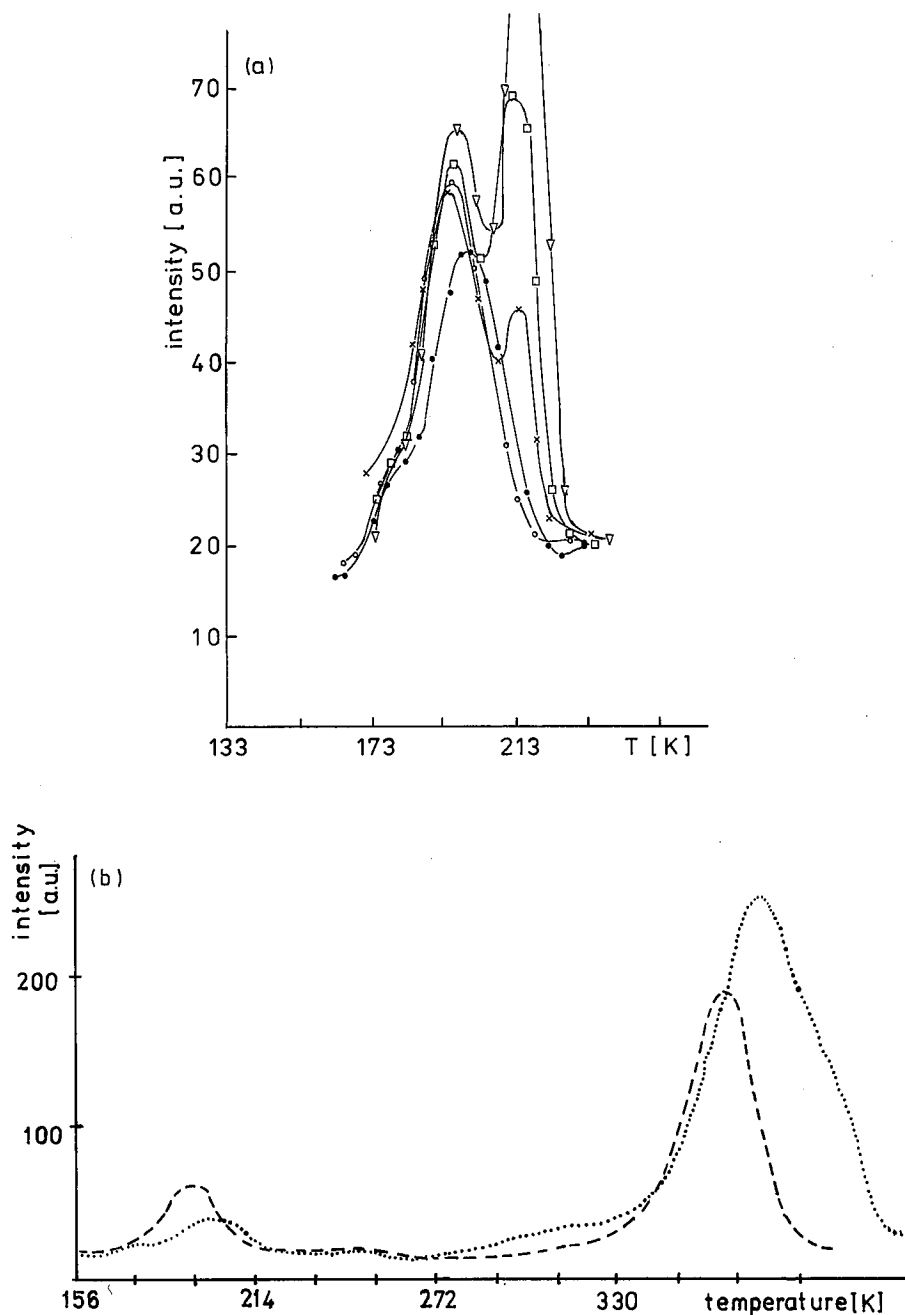


Fig. 6. The effect of solution treatment and RT ageing for M.1 (a) and M.2 (b) crystals; $T_p \cong RT$, $T_f = 178$ K, $V_p = 10^3$ V. The bands were obtained for AR (●), ST (▽) and RT stored samples (□, ×, o, -).

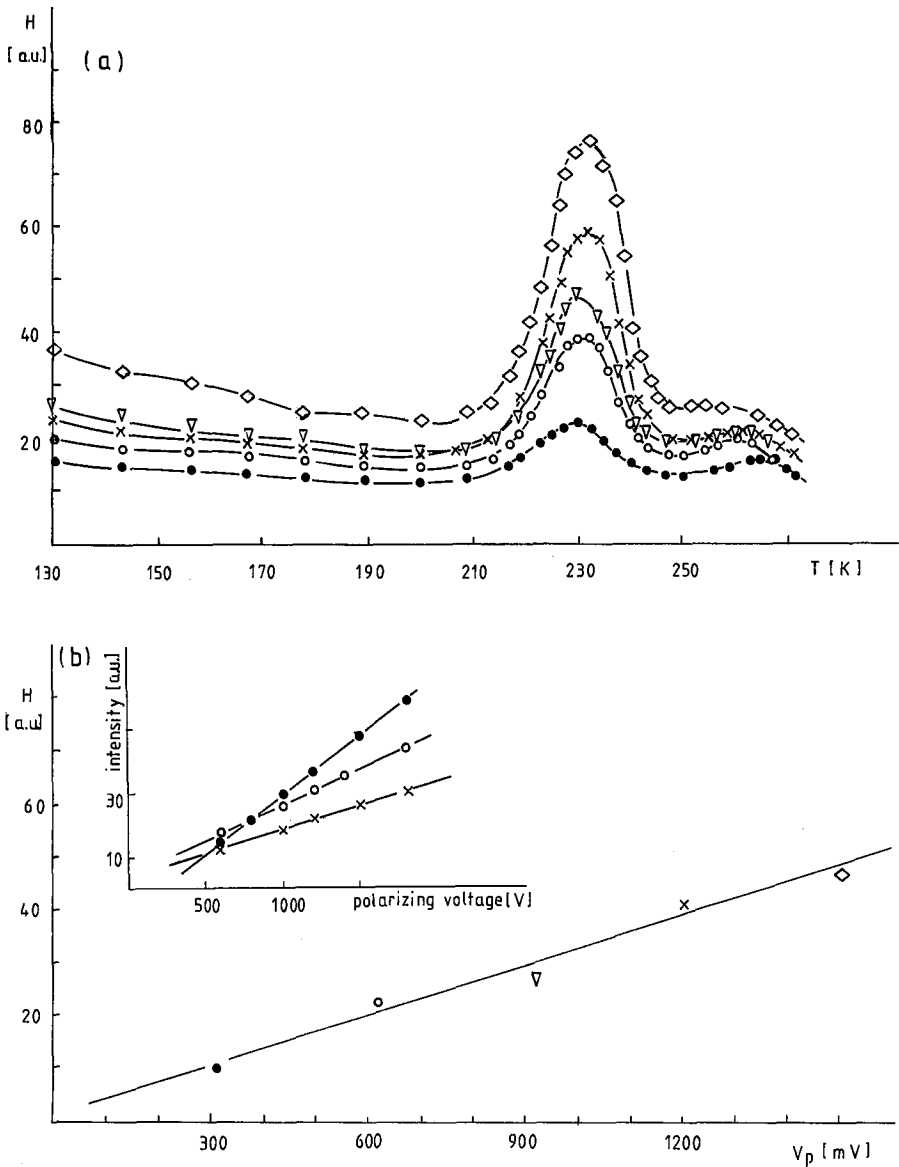


Fig. 7. Effect of V_p upon the dipolar band (a) and the relationship between H and V_p (b) for R.1; $T_p = 228$ K, $T_i = 209$ K. The inset of (b) shows the $H(T_p)$ plots for E.6 (\bullet), M.1 (\circ) and D.2 (Δ) crystals; in this case $T_p \cong RT$, $T_i = 178$ K.

dipoles satisfactorily accounts for the experimental observations. Some differences — with respect to the $AH:Me^{2+}$ crystal systems — were also detected in the high-temperature region. For instance, no simple concentration dependence was observed neither for the amplitude of the high-temperature band H^C nor for the

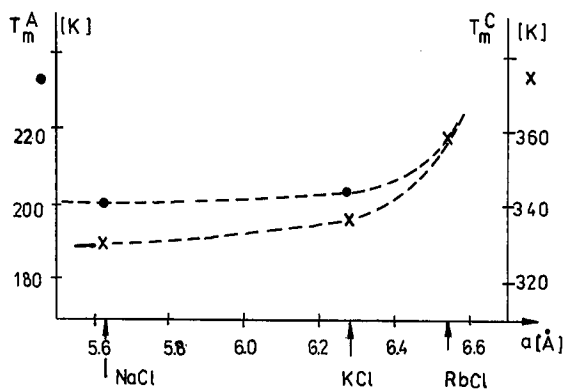


Fig. 8. Empirical relation between the peak positions of the low- (T_m^A) and high- (T_m^C) -temperature bands and the lattice parameter a of NaCl, KCl and RbCl crystals.

position of its maximum T_m^C ; on the other hand, the width of this band increases with the increasing content of bismuth.

3.3.2. Effects related with the solution treatment and plastic deformation

Water affinity of trivalent bismuth is responsible for the presence of some quantity of BiO^+ ions in freshly cutted NaCl samples annealed in air at high temperatures. This results in strong overlapping of the low-temperature band with relaxations of defects containing the oxygen-like ions.

Prolonged annealing (up to about 3.5 h) at 873 K of $\text{RbCl}:\text{Bi}^{3+}$ samples results in the increase in the low-temperature band at the expenses of the high-temperature one. Such conversion of bands was not detected previously, neither for Me^{2+} doped alkali halides [10] nor for Me^{3+} doped silver halides [5]. Because some of the mixed bismuth-potassium salts are chemically very stable, the re-solution of precipitated phases present in the AR $\text{KCl}:\text{Bi}^{3+}$ samples is not a simple task. It was stated, for instance, that the low-temperature ITC band remains unchanged after prolonged (3.5 h) high-temperature annealing. A peculiar reaction of the considered relaxations was observed for plastically deformed samples. For example, compression of the BiO^+ doped NaCl crystals results in the appearance of an additional low-temperature band positioned below the main dipolar one. Its amplitude H decreases with the storage at RT, and 48 h is enough for complete disappearance of this band. On the other hand, few percent of compression induces strong decrease in the high-temperature band amplitude, a distinct shift of its position towards higher values and a drastic increase in the bandwidth. Although some of these phenomena resemble the behaviour of the C band for $\text{AH}:\text{Me}^{2+}$ systems, interpretation of the obtained results cannot be done in terms of polarizations related with the classical Cottrell atmosphere. In contrast to divalent ions, whose ionic radius is comparable with that of the matrix, the small trivalent impurities are segregated near dislocations probably in the form of aggregates and/or precip-

itates which transform into simpler defects during both thermal and mechanical treatment of samples.

4. Summary

1. Optical absorption spectra of Bi^{3+} ions are similar to those typical of other heavy-metal ions with the s^2 electronic configuration; hence, the absorption can be exploited for analytical purposes.

2. Strong water affinity of trivalent bismuth and preferential bonding between Bi^{3+} and O^{2-} ions are responsible for the formation of BiO^+ molecular ions under conditions of crystal growth and during the high-temperature annealing of samples.

3. Exceptionally small solubility of the dopant can be observed, among others, in small differences of conductivity between the doped and nominally pure samples.

4. The charge compensating elements (either cation vacancies or the oxygen-like ions) together with trivalent bismuth give centres endowed with electrical moment; the reorientation of these "dipoles" can be monitored by the ITC technique.

5. The composed character of the impurity related defects is reflected in the complexity of all ITC spectra observed.

References

- [1] R. Capelletti, M.G. Bridelli, M. Friggeri, G. Ruani, in: *Proc. 5th Symp. Electrets, IEEE, Heidelberg (Germany) 1985*, IEEE, New York 1985, p. 294.
- [2] M. Hartmanova, E. Mariani, M. Lebl, *Czech. J. Phys. B* **22**, 623 (1972).
- [3] M. Hartmanova, M. Lebl, E. Mariani, *Cryst. Lattice Defects* **4**, 287 (1973).
- [4] S. Radhakrishna, A.M. Karguppikar, *J. Phys. Chem. Solids* **34**, 1497 (1973).
- [5] I. Kunze, P. Müller, *Phys. Status Solidi* **38**, 271 (1970).
- [6] R. Voszka, I. Tarjan, L. Berkes, J. Krajsovszky, *Krist. Technik* **1**, 423 (1966).
- [7] R. Fleischer, *Acta Metal.* **9**, 996 (1961).
- [8] E. Orowan, in: *Proc. Symp. Internal Stresses in Metals and Alloys*, University Press, London 1948, p. 451.
- [9] C. Bucci, R. Fieschi, G. Guidi, *Phys. Rev.* **148**, 816 (1966).
- [10] M. Suszyńska, R. Capelletti, *Cryst. Res. Technol.* **19**, 1489 (1984).
- [11] A. Fukuda, *Sci. Light (Tokyo)* **13**, 64 (1964).
- [12] M. Suszyńska, M. Hartmanova, H. Rezabkova, M. Lebl, *Czech. J. Phys. B* **26**, 1011 (1976).
- [13] F. Beniere, R. Rokbani, *J. Phys. Chem. Solids* **36**, 1151 (1975).
- [14] Gh. Stoicescu, S.V. Nistor, C.D. Mateescu, *Phys. Status Solidi B* **156**, 411 (1989).